Effect of Respirophasic Displacement of the Inferior Vena Cava on Size Measurement in 2-D Ultrasound Imaging

Effects of respirophasic displacements of inferior vena cava on size measurements from two dimensional ultrasound imaging

Piero Policastro[a], Leonardo Ermini[b], Stefania Civera[c], Stefano Albani[c,*], Giuseppe Musumeci[c], Silvestro Roatta[b], Luca Mesin[a,**]

[a]*Mathematical Biology and Physiology, Department of Electronics and Telecommunications, Politecnico di Torino, 10129 Turin, Italy; piero.policastro@polito.it (P.P.); luca.mesin@polito.it (L.M.)*
[b]*Department of Neuroscience, University of Torino, c.so Raffaello 30, 10125, Turin, Italy; leonardo.ermini@unito.it (L.E); silvestro.roatta@unito.it (S.R)*
[c]*Division of Cardiology, Ospedale Ordine Mauriziano di Torino, 10128, Turin, Italy; stefy.civera@gmail.com (S.C.); albani.aosta@gmail.com (S.A.); giuseppe.musumeci@gmail.com (G.M.)*

Abstract

Objective. The assessment of the volume status of a patient by ultrasound (US) imaging of inferior vena cava (IVC) is important for diagnosis and prognosis of different clinical conditions. To improve the clinical investigation of IVC, mainly based on unidirectional US (in M-mode), automated processing of two-dimensional US scans (in B-mode) allowed the possibility to track the tissue movements on the visualized plane and to average across different directions. However, the geometry of the IVC outside the visualised plane is not under control and could result in errors that have never been evaluated.

*Division of Cardiology, Umberto Parini Regional Hospital, 11100, Aosta, Italy;albani.aosta@gmail.com

**Corresponding Author: Luca Mesin, Dipartimento di Elettronica e Telecomunicazioni, Politecnico di Torino, Corso Duca degli Abruzzi, 24 - 10129 Torino - Italy; Email, luca.mesin@polito.it; Phone, +39 011.090.4085

Methods. We use a method, which integrates information from long and short axis views of IVC (simultaneously acquired in X-plane), to assess the problems in the estimation of IVC diameter by 2D US scans from 8 healthy subjects. Results. The relative movements between US probe and IVC induced the following problems when assessing the IVC diameter by 2D views: median error (i.e., absolute difference with respect to diameter measured in X-plane) of 17% using 2D US scans in long axis view of IVC affected by medio-lateral displacements (median of 4 mm); 7% and 9% of median error when measuring the IVC diameter from a short axis view in the presence of pitch angle (median of 0.12 radians) and cranio-caudal movement (median of 15 mm), respectively. Conclusion. Relative movements of IVC which are out of view of B-mode scans cannot be detected and cause problems in the estimation of IVC diameter.

Keywords: Inferior vena cava, Ultrasound, Tracking

Introduction

Ultrasound (US) scanning is an important medical imaging method due to its non-invasiveness and cost-effectiveness [1][2]. In recent years, this imaging technique has gained remarkable importance in medical structures due to the increased performance of the machines, e.g., in terms of spatial [3] and temporal resolution [4]. X-plane (or biplane) recording allows physicians to simultaneously acquire images of the same tissue in two perpendicular planes, enabling accurate analysis of complex structures [5].

Veins are blood vessels that return blood to the heart. They have a low internal pressure and are characterized by a prominent ability to dilate (i.e., they have a great compliance) and may thus accommodate and eventually redistribute large volumes of fluid [6]. Both arteries and veins have three layers, but arteries have a thicker middle layer to cope with higher blood pressure. Veins are thinner and less stiff, so they are more likely to change shape due to variations of the transmural pressure.

The inferior vena cava (IVC), the biggest vein vessel in the human body, is linked directly to the right atrium. The diameter variations of IVC show important information about the volume status of the subject and the central venous pressure [7];[8]. Specifically, the caval index (CI) is commonly used to assess IVC collapsibility, which correlates with the volume status [9] and the right atrial pressure [10]. It is obtained by measuring the maximum and minimum diameters of IVC [11]. However, the assessment of IVC size (and hence also the evaluation of CI) is not standardized [12], so that the measured values could be subject to errors [13]. As a consequence, poor accuracy is achieved when IVC indexes are used to estimate volume responsiveness [14]

and right atrial pressure [15]. Some causes of error are related to the following factors.

1. The use of an M-mode visualization, which selects a fixed US line, making the method prone to respirophasic IVC movements [16, 17].
2. The different modalities of respiration of the patients [18].
3. The experience of the operator [13].
4. The complicated geometry of the IVC and varying collapsibility in different directions along its longitudinal axis [19] and cross-section [20].
5. The three dimensional (3D) movement of the IVC relative to the US probe orientation, including both cranio-caudal and medio-lateral displacements [11], together with rotations in different planes [21].

Several algorithms have been developed for IVC segmentation to address some of these challenges. These algorithms analyse a single IVC view in B-mode, either longitudinal or transversal to the blood vessel [17, 22, 23]. The visualization in X-plane allows the identification of movements of IVC in the longitudinal and transverse directions at the same time [21]. An algorithm that integrates information from longitudinal and transverse views of the IVC to compensate for motion that adversely affects measurements from a single B-mode scan is described in [21]. In the simulated videos, this algorithm showed impressive performance in mean diameter estimation (with maximum error of 2% relative to the simulated ground truth), correctly compensating for the artefacts caused by the relative movements between IVC and probe.

Here, we document the error in the estimation of IVC size when using US scans from a single view in the presence of specific IVC movements, using as reference the algorithm compensating for them [21].

Specifically, we focus on the following important IVC displacements: medio-lateral translations, rotation in the longitudinal plane (measured by the pitch angle) and longitudinal translations. Notice that the reference algorithm, integrating long and short axis views of the IVC, was tested on simulated videos in which there was a single vein movement at a time [21]. In real US acquisitions, the three movements can be overlaid and concurrent with a change in vein size. Therefore, predicting the effect of each individual factor in an experimental setting is not trivial.

Thus, the aim of this paper is to analyse real data and assess the effects of specific IVC movements on the estimation of its size using US scans from individual B-planes. In fact, there are IVC movements that cannot be appreciated on the single 2D view. However, simultaneously monitoring the IVC position and movements on a second 2D plane perpendicular to the first one allows to detect and correct (in part) the possible errors in diameter assessment from single 2D views. Thus, the error in IVC size monitoring from single 2D views (related to IVC movements which are visible only out of the plane of view) is quantified using as reference the new algorithm [21], which integrates information from long and short axis views, acquired by X-plane scans.

Materials and Methods

We enrolled 8 healthy subjects. The Ethics Committee of Mauriziano Hospital (Turin) approved the study (approval number 388/2020; experimental protocol identifier v.1, June 1^{st} 2020), and informed consent was obtained according to the policies of the institutional review board. Anonymization

was applied to protect patient data. For each patient, an X-plane US video, which provides two simultaneous views of the same target in perpendicular US planes, was acquired using GE Vivid E95 (GE Healthcare, Vingmed Ultrasound, Horten, Norway). The output of the segmentation algorithms in long [19] and short axis [20] was provided as input to our 3D estimation algorithm (implemented in Matlab, the Mathworks, Natick, Massachusetts, USA) to extract IVC size from the combination of the two views [21].

Analysis of data and management of outliers

Diameters were estimated for each frame of the acquired US videoclips, using either of the following 3 methods.

1. Long-axis views: average of estimations along the IVC course in direction orthogonal to the axis, as in [19].
2. Short axis view: equivalent diameter estimated from the cross-sectional area of the IVC, as in [20].
3. X-plane: method proposed in [21], that integrates the information from long and short axis views.

Then, the differences between the estimations obtained from the 2D views (either in long or short axis) and those given integrating them (using the X-plane) were investigated as a function of different movements of the IVC with respect to the probe: transverse translation, pitch angle and longitudinal displacement.

Some diameter estimations, when displayed in relation to specific IVC movements, showed a large deviation from the main trend. This could be

due either to noisy frames determining mistakes in the processing or to peculiar relative locations of the probe with respect to the IVC, e.g., a great influence of the other geometrical parameters or an out-of-plane rotation. In fact, different tissue movements (translations, rotations, etc.) and deformations (collapsibility) occur together in experimental data. These particular diameter estimations were considered outliers and removed, as they could affect the interpretation of the effect of the specific geometrical parameter of interest. We identified the outliers by the isolation forest algorithm [24]: binary trees were used to isolate the data and those requiring fewer splits were given higher anomaly scores; outliers were identified as the 10% of data with largest anomaly scores.

Tests

The effect of three possible IVC movements, measured individually and correlated with diameter estimation error, have been investigated.

1. Medio-lateral translations. The movements of the IVC are easily visible in the transverse section, but they are not noticeable in the long axis view, where they induce an underestimation bias in the size which is more important as the section is further from the centre of the vein.
2. Variation of the value of the pitch angle. It can be compensated in the longitudinal section by IVC tracking. On the other hand, it is not visible in the short axis view and it has the effect of overestimating the transverse diameter (with a larger effect when the section is further from being orthogonal to the IVC axis).
3. Longitudinal translations. They are noticeable in the longitudinal section, where they can be compensated by IVC tracking. An error in

diameter estimation is found in the transverse view, if the size of the vein changes along its longitudinal course.

Using as reference the diameter estimated by integrating information from the long and short axis views (referred to as 'equivalent 3D diameter'), the percentage errors when using the 2D measurements (i.e., in long or short axis view) were computed as

$$error_{long} = 100 \times \frac{equivalent\ diameter_{long} - equivalent\ 3D\ diameter}{equivalent\ 3D\ diameter} \quad (1)$$

$$error_{transv} = 100 \times \frac{equivalent\ diameter_{transv} - equivalent\ 3D\ diameter}{equivalent\ 3D\ diameter} \quad (2)$$

where $equivalent\ diameter_{long}$ and $equivalent\ diameter_{transv}$ are the measurements obtained by averaging the diameters estimated in the long axis view (in different locations along the IVC course, in direction orthogonal to the axis, as in [19]) and in the short axis view (obtained from the cross-section area, as in [20]), respectively.

Analysis of the results

The percentage errors of the 2D versus 3D equivalent diameters (estimated for each frame of the US scans) were displayed in scatter plots, showing their relation with the three investigated IVC movements. Data (after excluding outliers) were interpolated with a line, indicating the standard error (SE).

Moreover, the ranges of observed movements and maximal percentage errors were investigated.

Given the equivalent diameter obtained by either of the 3 methods, the caval index (CI), the respiratory CI (RCI) and the cardiac CI (CCI) have been

computed (as in the previous work [13]). For each time series of equivalent diameter, more indexes have been estimated (i.e., CI and RCI were estimated for each respiratory cycle, CCI was computed for each heartbeat). Then they were averaged, obtaining single values (for all time series of equivalent diameter) which were compared.

Finally, the mean diameters and collapsibility indexes were explored and their possible differences among estimation methods (i.e., 2D long and short views or X-plane) were investigated by the Wilcoxon signed rank test for paired comparisons.

Results

We studied the contribution of three geometrical factors to the errors in IVC diameter estimation using longitudinal and transverse views. Each of these factors is here examined in detail, showing first specific examples (in Figures 1-3) and then the overall results (in the following figures).

Figure 1 shows a subject characterized by prominent medio-lateral movements of the IVC and for whom the diameters estimated by different methods differ significantly. Two frames are selected for which the displacement of the longitudinal plane from the IVC centre was either the smallest or the largest. At the bottom of the figure, the three estimated diameters are displaced over time. The corresponding time of the two frames reported above has been highlighted. The difference between the diameters estimated from the long axis, short axis and X-plane views was minimal when the centre of the IVC was close to the tilt line indicating the long axis section, but it was significant at maximum translation. The equivalent 3D diameter is estimated

compensating for the medio-lateral translation by using the short axis view. Thus, we can assume that it is not affected by the medio-lateral translation, contrary to the longitudinal diameter, which behaves very differently from the estimation from the cross-section when the displacement is large.

The effect of the estimated IVC rotation in the long axis plane (i.e., the pitch) on diameter measurement is shown in Figure 2. Again, two frames were selected to show different conditions: the first where the longitudinal axis of IVC shows some pitch angle with the tilt line indicating the direction of the short axis section and the second in which they are almost perpendicular. Due to the pitch angle visible in the longitudinal view, the cross-section is larger than when it is taken orthogonal to the IVC axis, so that the equivalent diameter estimated from the short axis view has a positive bias, as shown in the traces reported in the lower part of the Figure. The equivalent diameter obtained processing the two sections from the X-plane view compensates the effect of this error. Notice that, when the transverse section is orthogonal to the IVC axis (i.e., for the second frame), the three estimated diameters are almost identical.

The third case, i.e., longitudinal translation, is shown in Figure 3. An IVC with a conical shape, as for the subject chosen for this figure, emphasizes the effect of this cranio-caudal translation. Two frames were chosen in which the relative translation of the cross-section is quite large. The three estimations of the diameter (by 2D views in B-mode in long and short axis and X-plane) were almost identical for the first frame, but the translation largely affected the cross-section for the second frame.

From the specific examples in Figures 1-3, notice a common interesting

thread (that we'll find again later, in Figure 8, where the entire dataset is considered): the long axis view provides in general smaller estimates than the short axis, as the first can be biased negatively by a medio-lateral displacement, whereas the second is positively biased by a pitch rotation with respect to the IVC axis (both problems are not visible from the corresponding view, respectively).

Figures 4-6 show the overall results from the entire dataset, considering the same IVC movements as in the specific examples in Figures 1-3, respectively. The dynamics of the IVC is quite complex, as different translations and rotations occur simultaneously and together with the variation of size. Moreover, IVC movements and size variation are usually correlated, as they are both related to the respiratory cycle. Thus, to try to bring out the possible effect of specific movements on the diameters estimated from long and short axis views, they were referred to the value computed by the new algorithm (applied to X-plane US scans), that compensates their effects. Thus, the percentage error, given in either (1) or (2), is plotted versus the different movements.

Specifically, Figure 4 shows a scatter plot for each of the 8 subjects. The percentage error of the estimate of the diameter in long axis is given for each frame of the videos as a function of the relative medio-lateral displacement of the IVC from its centre with respect to the transverse diameter. Notice that a relative displacement was shown, as a dimensional translation (i.e., given in mm) has a different effect depending on the size of the cross-section. Considering also that the diameter of the IVC can vary substantially between subjects and due to IVC collapsibility, only displacements relative to IVC size

can fairly demonstrate their effect.

In Figure 5, the percentage error in the estimation of the diameter from the short axis view is shown in scatter plots (one for each subject) versus the pitch angle in radians (with zero corresponding to a tilt line orthogonal to the IVC axis). A positive bias in the estimation of IVC size from short axis is expected when the pitch angle is further from zero. Note that there is sometimes an offset, which indicates an error even when the pitch angle is close to zero. Since the short-axis view does not have access to the longitudinal cross-section information, there may be changes outside the cross-section plane that account for the observed bias. For example, the null pitch condition could apply when the IVC is shifted to a region where it is on average larger or smaller than its average size in the region analysed by the 3D approach.

In Figure 6, scatter plots for each subject are shown with the longitudinal translation (mm) on the x-axis (considering as positive the translations toward the region in which the dimension of the IVC was larger in the average across the frames of the echography) and on the y-axis the percentage error in the estimation of the diameter from the short axis view.

Figure 7 shows the ranges of the three different movements and the maximum errors observed in the subjects. Respiratory cycles are the principal cause of IVC movement, with the greatest excursion range occurring between inspiration and expiration. We expect that the maximum errors occur at the maximum excursions of the movements: this is the rationale of relating the maximum errors with the range of movements. Parameters were computed as 90% percentiles (after removing outliers), to get robust estimations.

The pitch angle has never been documented before: it is a small rotation, but it can have a discreet effect when taking measurements with a short axis view. The median maximal errors are around 17% for the long axis measurement affected by a medio-lateral movement; when using the short axis view, it is about 7% and 9% for the pitch angle and cranio-caudal translation, respectively. The median cranio-caudal and medio-lateral translations were 15 and 4 mm, respectively, and the median pitch angle was 0.12 rad.

The repercussions of using a 2D scan (in long or short axis view) instead of a 3D scan (X-plane view) on the estimation of parameters of clinical interest are shown in Figure 8. As already noticed in the first figures, the IVC diameter tends to be underestimated in long axis view, whereas it is overestimated when using the short axis view (both variations with respect to the X-plane estimation are statistically significant, according to the Wilcoxon signed rank test; notice that the diameter estimated in short axis is always the largest, giving high significance in paired comparisons). The collapsibility indexes appear to have less consistent variations, even if in the average there is a small (not significant) positive bias in measuring the CI and RCI in long axis view versus the 3D approach. The estimations by the long axis view of CI and RCI have also a quite large variation with respect to using the 3D information provided by the X-plane view. In fact, the range of the differences is about 20% (notice that the median CI is about 25% and 33% for the X-plane and long axis views, respectively, with the result that the uncertainty is a rather large amount of the value to be measured). Instead, the range of differences in CI and RCI estimations is about 10% for the short axis view. The CCI shows lower estimation differences, but also the range of

values to be measured is smaller.

Discussion

IVC shows large movements during respiration, as it is attached to the diaphragm and adhered to other tissues. Moreover, the skin surface over which the probe is placed is also affected by large respirophasic movements. Achieving the US scan of a particular area during the respiratory cycle can be challenging. In fact, while B-mode visualisation and image processing techniques can compensate for in-plane movements, the 3D geometry and movements of IVC can also develop partly outside the scanned view.

In this paper, we used the visualization in X-plane to detect and compensate the IVC spatial orientation and movements. Using the X-plane as reference, we documented the measurement errors expected in simple 2D visualization (in either short or long axis).

Figure 1 clearly shows the effect of the medio-lateral translation on the diameter estimated from the longitudinal view. The effect of this movement can be mitigated when integrating information from the short axis view. It is mainly caused by breathing, as the abdomen (on which the probe is placed) is moving, so that it is not easy to maintain the IVC axis on the 2D longitudinal plane, by manually adjusting the probe orientation. In fact, the IVC is collapsing at the same time in which it is moving, so that it is not easy from a long axis view to discriminate if the size changes are attributable only to collapsibility or to a medio-lateral displacement.

In the lower graph of Figure 1, the diameters estimated from the three different sources are almost the same at point 1 (when the tilt plane in the

transverse plane is close to the centre of the cross-section), but there are some differences at point 2. In fact, at the second selected point, the transverse section line was close to the vein wall. If the movement is greater than the cross-section radius, it can also cause the vein to disappear in the longitudinal view (leading the operator to suspect a complete collapse).

An important pitch rotation of the IVC in the plane of the long axis is seen only in few subjects involved in this study. However, its effect is clearly that of deforming the visualized cross-section. For example, in the ideal case in which the IVC is a cylinder with circular section, the visualized cross-section is an ellipse with larger eccentricity as the angle increases. Figure 2 shows this problem, considering two frames in which the short axis section is either close or far from being orthogonal to the IVC axis.

The cranio-caudal movement of IVC is the most evident during respiration, as the vein is attached to the diaphragm. However, it has an important effect on the estimation of IVC size from the cross-section only if the vein presents substantial size changes along its length (or if it is associated to a pitch rotation). Figure 3 shows an example of IVC with size changes along its course: as the short axis section is fixed, the cranio-caudal movement causes the US plane to intersect the vein at different sites, thus producing only apparent size changes. The integration of the information from the two sections allows the new algorithm based on X-plane view to compensate for this problem.

From the quantitative point of view (Figures 4-6), the detected medio-lateral (Figure 4) and cranio-caudal movements (Figure 6) are compatible with [11]. The pitch angle, however, was never documented in the litera-

ture.

The interpretation of the results must be done with caution, as the different movements and size variations occur together and may be correlated. In addition, it is possible that some frames were taken out of the plane (i.e., at a yaw angle), causing the reference algorithm (based on the X-plane view) to also fail. In fact, in few cases, the results were different from those expected. However, the average behaviour across subjects is in line with our expectations, easily interpreted in simulated conditions [21], i.e., underestimation of the diameter in long axis in case of medio-lateral translation and overestimation in short axis for large pitch angles and cranio-caudal translations toward a region in which the IVC is larger. This is found in the overall results shown in Figure 7. It summarises the magnitude of each movement investigated, showing the distribution of the values observed on the subjects included in the study. The three movements are considered in different panels, showing the scatter plots of the maximal percentage error versus the range of movements and the boxplots of each variable. The median errors (about 17% for the long axis measurement with medio-lateral movement; 7% and 9% in short axis for pitch angle and cranio-caudal translation, respectively) indicate some limitations in the accuracy with which the size of the IVC can be estimated using a single ultrasound section. This could have implications for the repeatability of measurements [13]. We expect that the observed errors could depend on the operator and on the subject (as indicated by the large ranges of variation), as they reflect different factors, as the IVC anatomy and the relative motion between the IVC (affected by the modality of respiration, tissue compliance, etc.) and the probe (handled by an operator

trying to accommodate abdomen movements during respiration). However, in the average, the errors have consistent dependencies on the movements, which are in line with the results of the theoretical part of our work [21]. In simulations, each movement could be considered separate from the others, one at a time, documenting its pure effect; in experimental data, other concomitant motions or deformations can obscure the interpretation of the results. However, still our experimental results confirm the simulations. In fact, it is clear that the estimation of IVC size is affected by movements not identifiable in a single plane of view. Thus, caution in the interpretation of measurements is recommended when measuring IVC using a 2D view. It is hoped that the increased use of US systems for X-plane visualization and 3D estimation will help to reduce errors and to limit measurement variability, which is still the most important limitation of this noninvasive assessment of IVC.

The problems in measuring IVC size using 2D US visualizations are reflected into the estimation of collapsibility indexes (as CI, RCI and CCI). The largest variability is found in the estimation of CI and RCI, that are directly affected by the respiratory cycle. Our data show some variability in the estimations, but not statistically significant differences with respect to the assessment in X-plane, nor a clear trend or bias. In fact, movements and size variations are correlated: thus, depending on the relative position of the probe and the IVC, the contributions to size changes from movement and respiration-induced pressure variations could add up or be in counter-phase. This introduces variations in the estimation of caval indexes from the different views which are not consistent across different subjects. This

could justify in part the poor repeatability of collapsibility assessment of IVC documented in the literature [13].

Given the problems in estimating IVC dynamics from 2D views (either in long or short axis), the 3D approach could be a potential useful alternative (if systems that provide visualization in the X plane become widespread). Assessing its benefits is left for future investigations. For example, it would be interesting to test the possible improvements in the definition of the clinical picture (e.g., in diagnosing the volume status or measuring the right atrial pressure) or the repeatability of the estimates obtained using the new algorithm processing the X-plane view.

Conclusions

The evaluation of IVC size from longitudinal and transverse views are affected by the vein movements that cannot be observed in the plane of the US scan. The problem can be mitigated by integrating the information from the two planes, synchronously acquired by an US system in X-plane. Specifically, the algorithm introduced in the article, previously published, is able to compensate for medio-lateral translation, mean longitudinal axis pitch and longitudinal translation. It was used as reference to document the effect of those movements in limiting the accuracy in evaluating IVC size and collapsibility in experimental data from single tilt sections. Specifically, this study for the first time simultaneously quantifies 3 movements of the IVC on experimental US scans and confirms the implications on the errors that characterize the 2D assessments.

Conflict of interest

An instrument implementing the 2D algorithms used in this paper was patented by Politecnico di Torino and Universitá di Torino (patent number WO 2018/134726) and was taken in license by VIPER s.r.l.

Data Availability Statement

Data are available from the corresponding author upon reasonable request.

References

[1] Lentz B, Fong T, Rhyne R, Risko N. A systematic review of the cost-effectiveness of ultrasound in emergency care settings. Ultrasound Journal. 2021;13(1):16.

[2] Zhang Y, Begum HA, Grewal H, Etxeandia-Ikobaltzeta I, Morgano GP, Khatib R, et al. Cost-effectiveness of diagnostic strategies for venous thromboembolism: a systematic review. Blood Adv. 2022;6(2):544-67.

[3] Hasegawa H. Improvement of range spatial resolution of medical ultrasound imaging by element-domain signal processing. Japanese Journal of Applied Physics. 2017 may;56(7S1):07JF02. Available from: https://dx.doi.org/10.7567/JJAP.56.07JF02.

[4] Ng A, Swanevelder J. Resolution in ultrasound imaging. Continuing Education in Anaesthesia Critical Care and Pain. 2011 08;11(5):186-92. Available from: https://doi.org/10.1093/bjaceaccp/mkr030.

[5] Convissar D, Bittner EA, Chang MG. Biplane Imaging Versus Standard Transverse Single-Plane Imaging for Ultrasound-Guided Peripheral Intravenous Access: A Prospective Controlled Crossover Trial. Crit Care Explor. 2021;3(10):e545.

[6] Mesin L, Albani S, Policastro P, Pasquero P, Porta M, Melchiorri C, et al. Assessment of Phasic Changes of Vascular Size by Automated Edge Tracking-State of the Art and Clinical Perspectives. Front Cardiovasc Med. 2022;8:775635.

[7] Albani S, Mesin L, Roatta S, De Luca A, Giannoni A, Stolfo D, et al. Inferior Vena Cava Edge Tracking Echocardiography: A Promising Tool with Applications in Multiple Clinical Settings. Diagnostics. 2022;12:427.

[8] Policastro P, Mesin L. Processing Ultrasound Scans of the Inferior Vena Cava: Techniques and Applications. Bioengineering. 2023;10:1076.

[9] Mesin L, Roatta S, Pasquero P, Porta M. Automated Volume Status Assessment Using Inferior Vena Cava Pulsatility. Electronics. 2020;9(10).

[10] Mesin L, Albani S, Sinagra G. Non-invasive Estimation of Right Atrial Pressure Using Inferior Vena Cava Echography. Ultrasound Med Biol. 2019;45(5):1331-7.

[11] Blehar DJ, Resop D, Chin B, Dayno M, Gaspari RB. Inferior vena cava displacement during respirophasic ultrasound imaging. Critical Ultrasound Journal. 2012;4(18):1-5.

[12] Wallace D, Allison M, Stone MB. Inferior vena cava percentage collapse during respiration is affected by the sampling location: an ultrasound study in healthy volunteers. Acad Emerg Med. 2010;17(1):96-9.

[13] Mesin L, Giovinazzo T, D'Alessandro S, Roatta S, Raviolo A, Chiacchiarini F, et al. Improved repeatability of the estimation of pulsatility of inferior vena cava. Ultrasound Med Biol. 2019;45:2830-43.

[14] Orso D, Paoli I, Piani T, Cilenti FL, Cristiani L, Guglielmo N. Accuracy of Ultrasonographic Measurements of Inferior Vena Cava to Determine

Fluid Responsiveness: A Systematic Review and Meta-Analysis. Journal of Intensive Care Medicine. 2020;35:354 363. Available from: https://api.semanticscholar.org/CorpusID:34815277.

[15] Magnino C, Omede' P, Avenatti E, Presutti DG, Iannaccone A, Chiarlo M, et al. Inaccuracy of Right Atrial Pressure Estimates Through Inferior Vena Cava Indices. The American journal of cardiology. 2017;120 9:1667-73. Available from: https://api.semanticscholar.org/CorpusID:27137870.

[16] Mesin L, Pasquero P, Albani S, Porta M, Roatta S. Semi-automated tracking and continuous monitoring of inferior vena cava diameter in simulated and experimental ultrasound imaging. Ultrasound Med Biol. 2015;41:845-57.

[17] Belmont B, Kessler R, Theyyunni N, Fung C, Huang R, Cover M, et al. Continuous inferior Vena Cava diameter tracking through an iterative Kanade-Lucas-Tomasi-based algorithm. Ultrasound in medicine & biology. 2018;44(12):2793–2801. Available from: http://dx.doi.org/10.1016/j.ultrasmedbio.2018.07.022.

[18] Folino A, Benzo M, Pasquero P, Laguzzi A, Mesin L, Messere A, et al. Vena cava responsiveness to controlled isovolumetric respiratory efforts. Journal of Ultrasound in Medicine. 2017;36(10):2113-23.

[19] Mesin L, Pasquero P, Roatta S. Tracking and Monitoring Pulsatility of a Portion of Inferior Vena Cava from Ultrasound Imaging in Long Axis. Ultrasound Med Biol. 2019;45:1338-43.

[20] Mesin L, Pasquero P, Roatta S. Multi-directional assessment of Respiratory and Cardiac Pulsatility of the Inferior Vena Cava from Ultrasound Imaging in Short Axis. Ultrasound Med Biol. 2020;46:3475-82.

[21] Policastro P, Mesin L. Estimation of Inferior Vena Cava Size from Ultrasound Imaging in X-Plane. Electronics. 2024:2024061272.

[22] Nakamura K, Tomida M, Ando T, Sen K, Inokuchi R, Kobayashi E, et al. Cardiac variation of inferior vena cava: new concept in the evaluation of intravascular blood volume. Journal of medical ultrasonics (2001). 2013;40(3):205–209. Available from: http://dx.doi.org/10.1007/s10396-013-0435-6.

[23] Sonoo T, Nakamura K, Ando T, Sen K, Maeda A, Kobayashi E, et al. Prospective analysis of cardiac collapsibility of inferior vena cava using ultrasonography. Journal of critical care. 2015;30(5):945–948. Available from: http://dx.doi.org/10.1016/j.jcrc.2015.04.124.

[24] Liu FT, Ting KM, Zhou ZH. Isolation Forest. 2008 Eighth IEEE International Conference on Data Mining. 2008:413-22.

Figure Captions

Figure 1: Estimation of the diameter of the inferior vena cava (IVC) in subject 5 in which the vein makes a large medio-lateral movement. The top panels display two X-plane echography images of IVC, in which the long axis section is taken either close to the centre of the cross-section (left) or close to the border (right). The time course of the diameter is shown in the bottom panel, estimated from the longitudinal and transverse views and by integrating their information. Two arrows, in the bottom graph, indicate the times in which the frames shown on top occurred. A small diameter is estimated from the long axis view when the medio-lateral translation is large.

Figure 2: Estimation of IVC diameter in subject 4 in which the vein makes an in-plane rotation. The top panels display two X-plane echography images of IVC, in which the angle between the short axis section and the vein is small (left) or close to 90° (right). The time course of the diameter is shown in the bottom panel, estimated from the longitudinal and transverse views and by integrating their information. Two arrows, in the bottom graph, indicate the times in which the frames shown on top occurred. The diameter estimated from a short axis view has a positive bias when the angle is smaller.

Figure 3: Estimation of IVC diameter in subject 1 in which the vein has large variations of the section in its long axis course. The top panels display two X-plane echography images of IVC, in which the translation of the vein makes the short axis section be taken either where it is

smaller (left - cranial direction) or larger (right - caudal). The time course of the diameter is shown in the bottom panel, estimated from the longitudinal and transverse views and by integrating their information. Two arrows, in the bottom graph, indicate the times in which the frames shown on top occurred. In this case, the diameter estimated from a short axis view has a positive bias when the IVC moves in caudal direction.

Figure 4: Percentage error of the diameter derived from the longitudinal section relative to the equivalent diameter recovered from IVC volume estimation, shown as a function of the medio-lateral translation. All frames and subjects are considered. The x-axis shows the ratio of the medio-lateral translation with respect to the tilt line to the diameter calculated from the transverse section. The linear interpolation is shown by a red line and the range defined by the standard error is indicated by a red dotted line, after removing the outliers. The identifier of the subjects, the standard error, and the slope of the interpolation line are indicated in the title.

Figure 5: Percentage error of the diameter derived from the transverse section relative to the equivalent diameter recovered from IVC volume estimation, shown as a function of the absolute value of the pitch angle. All frames and subjects are considered. The x-axis shows the pitch, in radians, with respect to the perpendicular tilt line. The linear interpolation is shown by a red line and the range defined by the standard error is indicated by a red dotted line, after removing the outliers.

The identifier of the subjects, the standard error, and the slope of the interpolation line are indicated in the title.

Figure 6: Percentage error of the diameter derived from the transverse section relative to the equivalent diameter recovered from IVC volume estimation, shown as a function of longitudinal translations. All frames and subjects are considered. The x-axis shows the longitudinal translations with respect to the tilt line (mm). The linear interpolation is shown by a red line and the range defined by the standard error is indicated by a red dotted line, after removing the outliers. The identifier of the subjects, the standard error, and the slope of the interpolation line are indicated in the title.

Figure 7: Range of movements and percentage errors (ErrL and ErrT indicating the error when using the long and short axis view, respectively) observed in different subjects (scatter plots of a pair of variables and boxplot of each variable). A) Error in the estimation of the diameter from the long axis view over the medio-lateral translation. For each subject, the maximal error (outlier excluded) and the maximal translation in mm are considered. A scatter plot and a boxplot of each variable are shown. B) Error in the estimation of the diameter from the short axis view over the pitch angle (same format as in A). C) Error in the estimation of the diameter from the short axis view over the cranio-caudal translation.

Figure 8: Estimation of IVC parameters (i.e., mean diameter, caval index (CI), respiratory caval index (RCI), and cardiac caval index (CCI)),

using US scans in X-plane (3D), long axis view (2D long) and short axis view (2D short). A) Individual parameters (mean diameter, CI, RCI and CCI) estimated from each subject using the 3 methods (3D, 2D long and 2D short). Statistical differences were found for the measurement of the diameter ($*$ $p<0.05$ and $**$ $p<0.005$)B) Box and whiskers plots (showing median, quartiles, range, and outliers) of the estimations of the parameters with the 3 methods. C) Box and whiskers plots of the difference in the estimations of the parameters when using the 2D methods instead of the 3D one.

Figure 4

Click here to access/download;Figure;Figure4.png

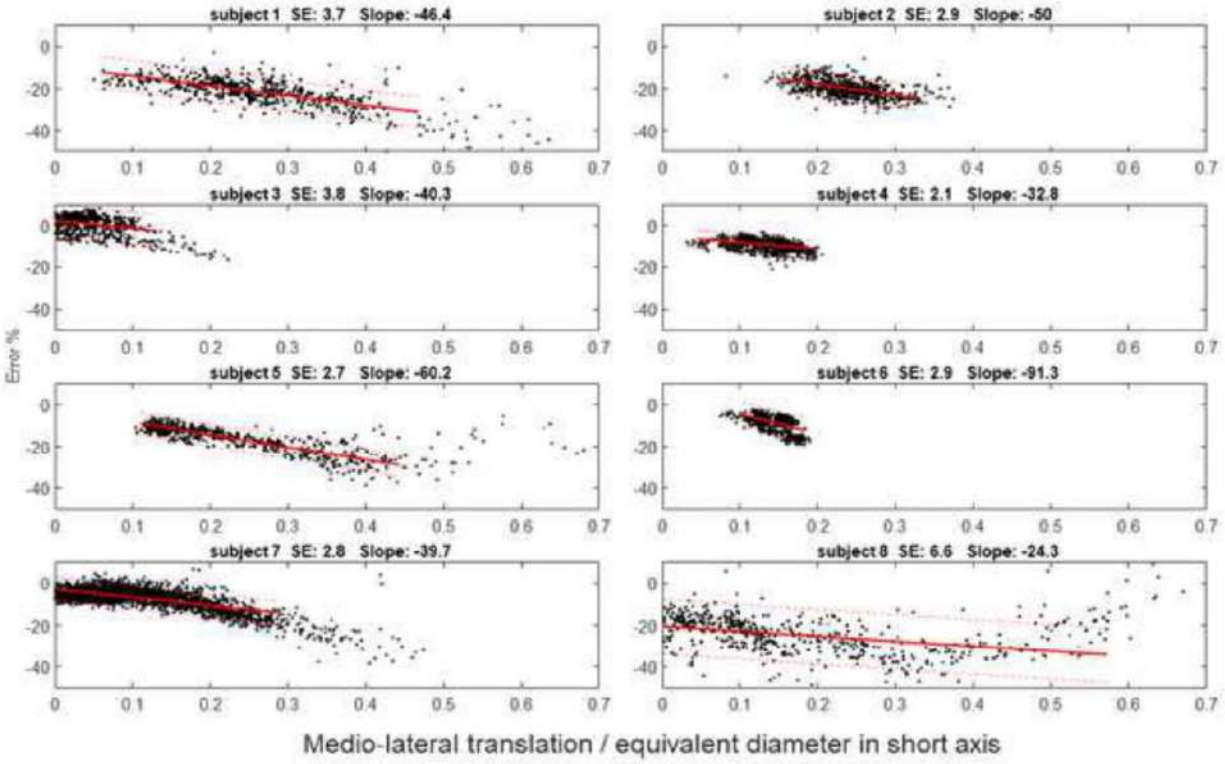

Figure 5

Click here to access/download;Figure;Figure5.PNG

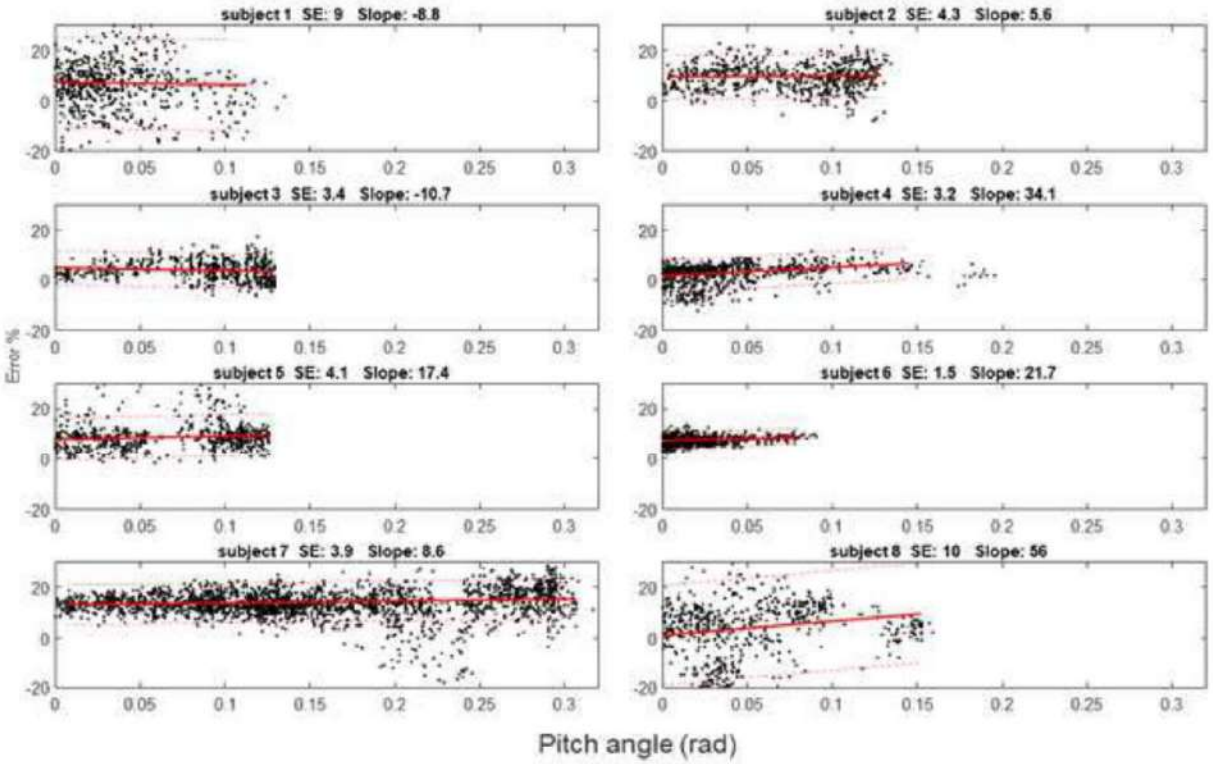

Figure 6

Click here to access/download;Figure;Figure6.PNG

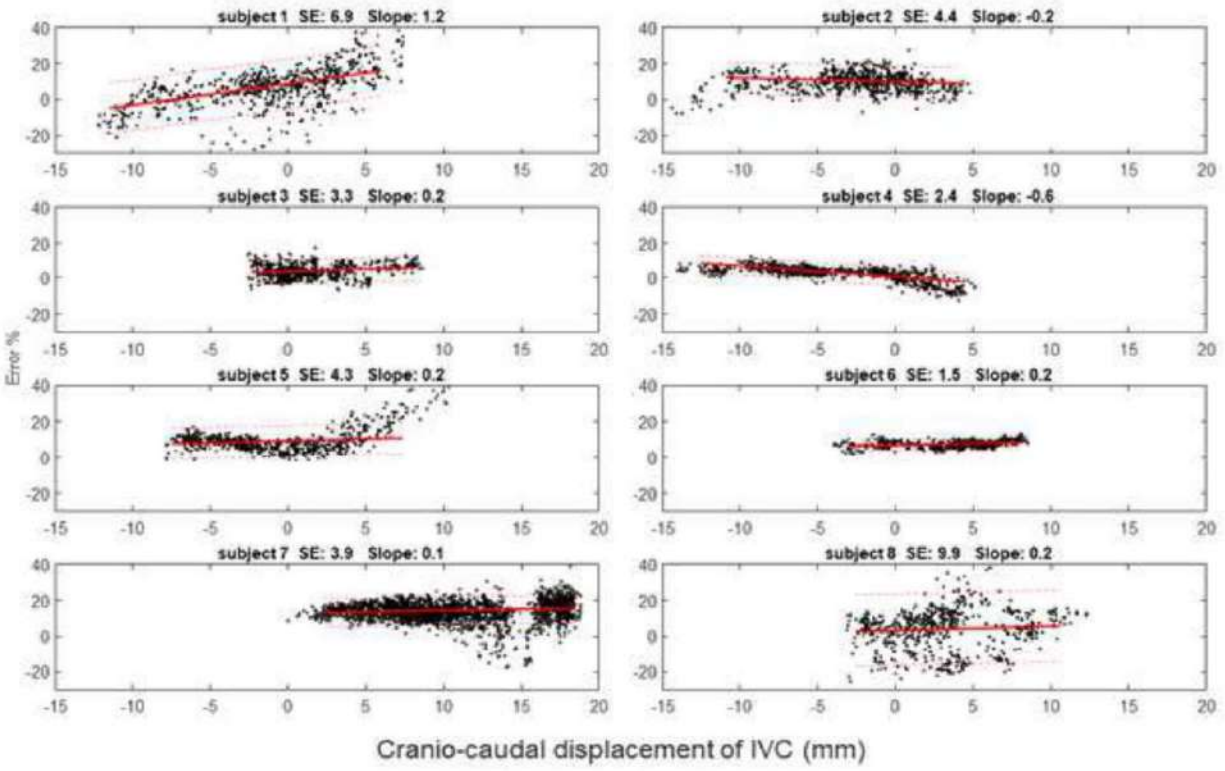

Figure 7

Click here to access/download;Figure;Figure7.png

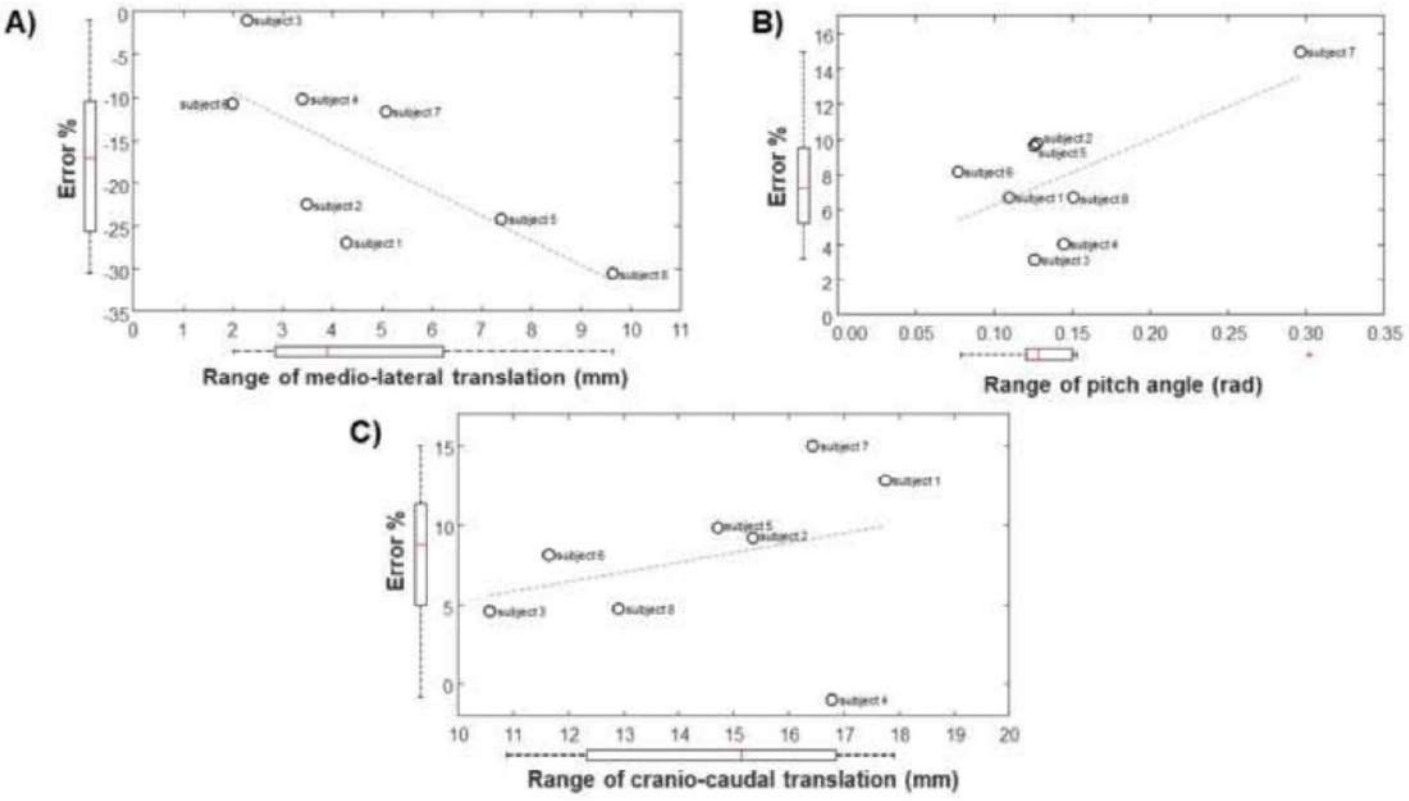

Figure 8

Click here to access/download;Figure;Figure8.png

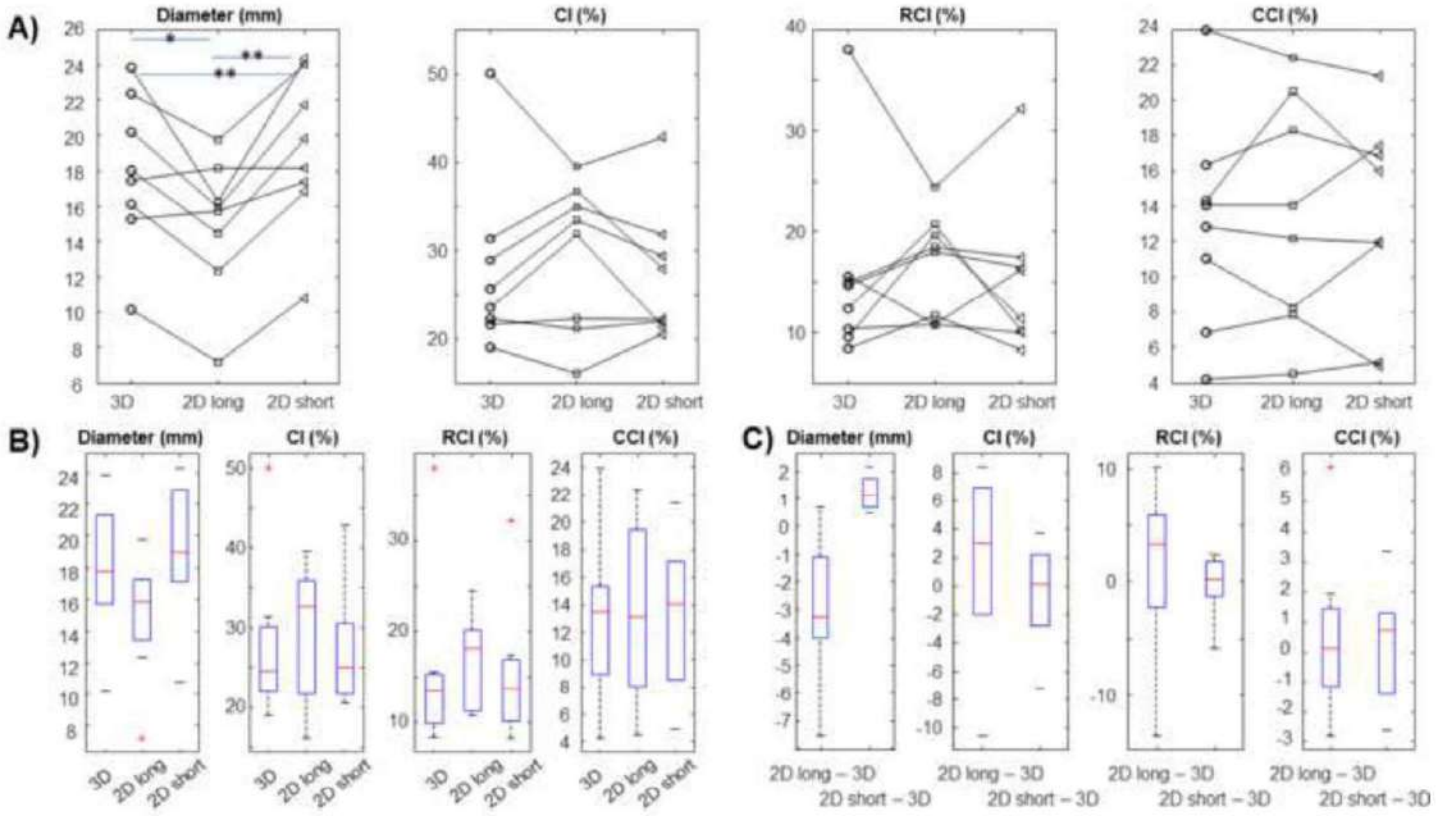

Figure 2

Click here to access/download;Figure;Figure2.PNG

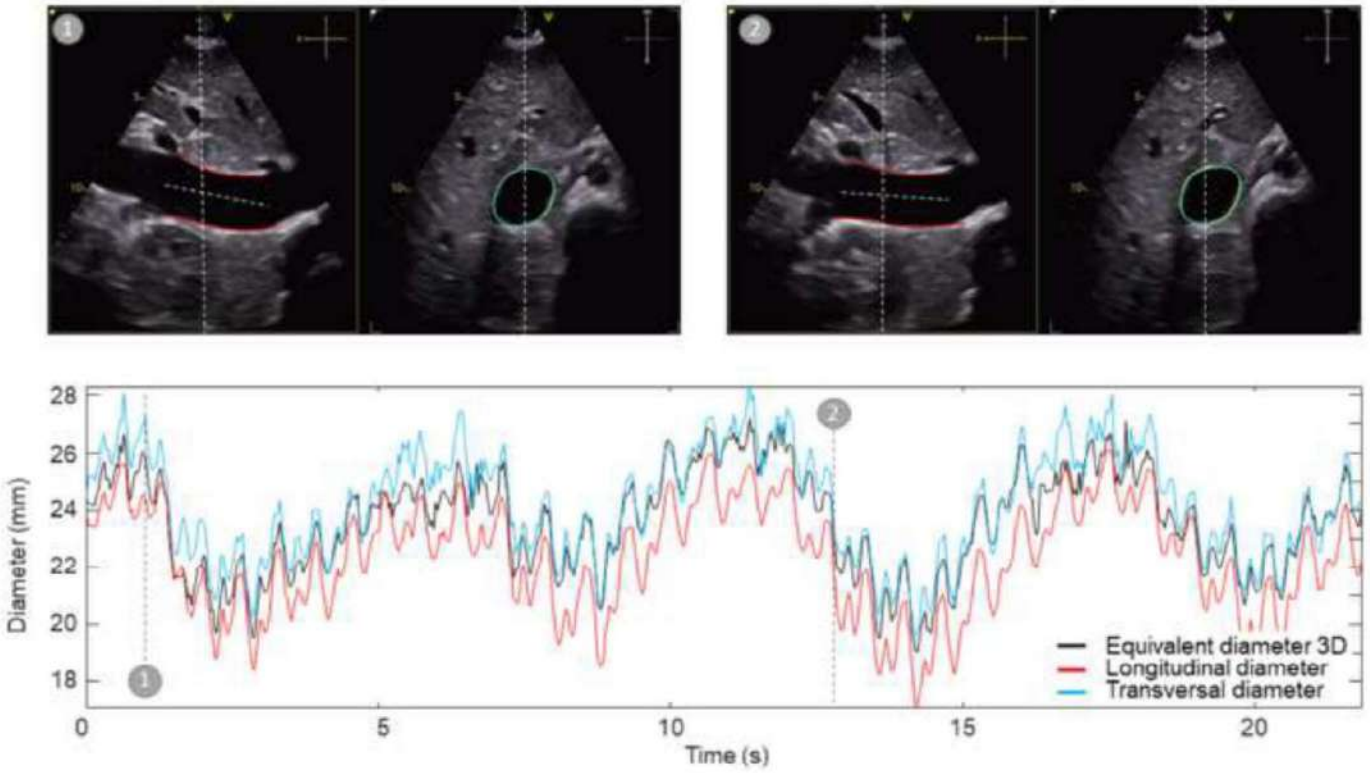

Figure 3

Click here to access/download;Figure;Figure3.PNG

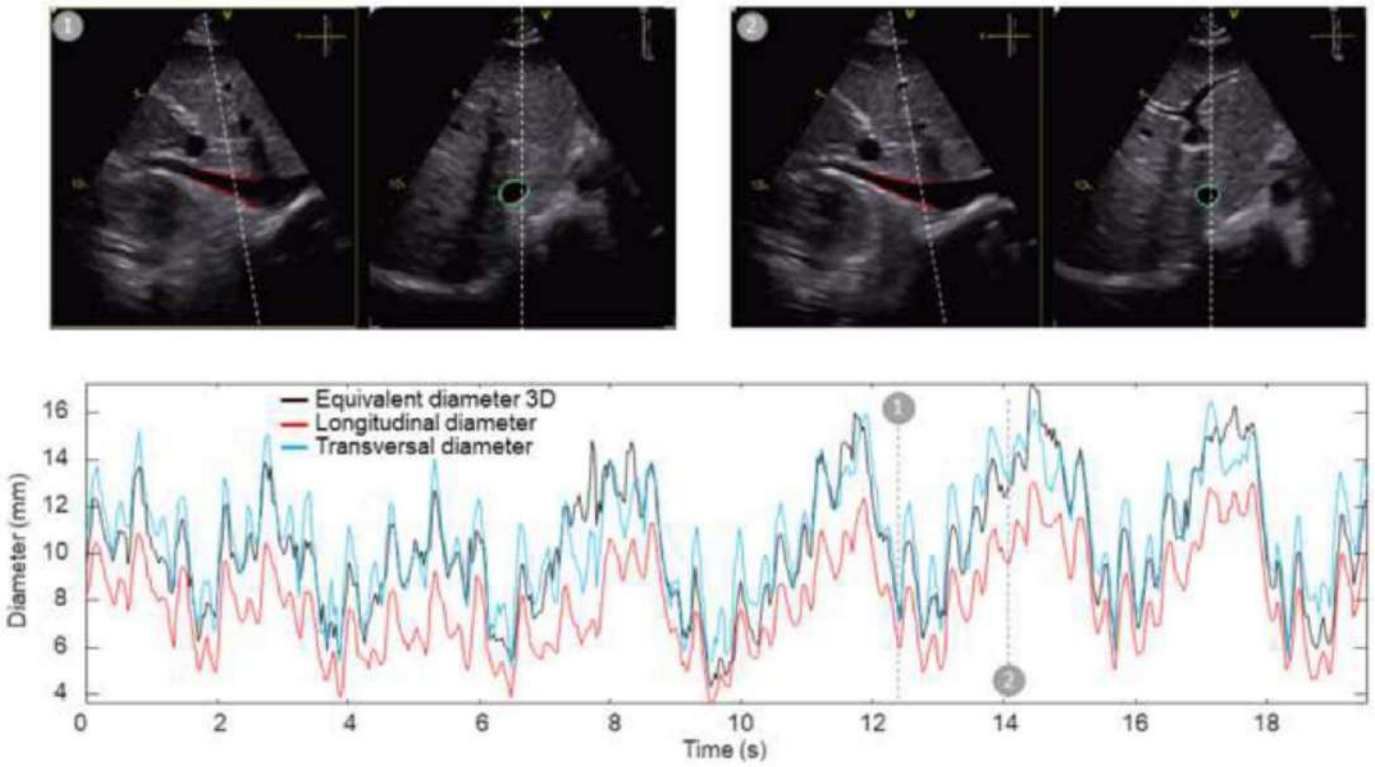

Figure 1

Click here to access/download;Figure;Figure1.PNG